Defence Technology 16 (2020) 316–324

Contents lists available at ScienceDirect

Defence Technology

journal homepage: www.keaipublishing.com/en/journals/defence-technology

Coating processes towards selective laser sintering of energetic material composites

Zetu Jiba [a, *], Walter W. Focke [b], Lonji Kalombo [c], Moshawe J. Madito [b]

[a] Council for Scientific and Industrial Research (CSIR), Defence Peace Safety and Security, P.O Box 395, Pretoria 0001, South Africa
[b] University of Pretoria, South Africa
[c] CSIR, Chemical Cluster, South Africa

ARTICLE INFO

Article history:
Received 2 April 2019
Received in revised form
12 May 2019
Accepted 21 May 2019
Available online 26 May 2019

Keywords:
Coating processes
Energetic materials
Simulants
Mock explosives
Additive manufacturing
Selective laser sintering

ABSTRACT

This research aims to contribute to the safe methodology for additive manufacturing (AM) of energetic materials. Coating formulation processes were investigated and evaluated to find a suitable method that may enable selective laser sintering (SLS) as the safe method for fabrication of high explosive (HE) compositions. For safety and convenience reasons, the concept demonstration was conducted using inert explosive simulants with properties quasi-similar to the real HE. Coating processes for simulant RDX-based microparticles by means of PCL and 3,4,5-trimethoxybenzaldehyde (as TNT simulant) are reported. These processes were evaluated for uniformity of coating the HE inert simulant particles with binder materials to facilitate the SLS as the adequate binding and fabrication method. Suspension system and single emulsion methods gave required particle near spherical morphology, size and uniform coating. The suspension process appears to be suitable for the SLS of HE mocks and potential formulation methods for active HE composites. The density is estimated to be comparable with the current HE compositions and plastic bonded explosives (PBXs) such as C4 and PE4, produced from traditional methods. The formulation method developed and understanding of the science behind the processes paves the way toward safe SLS of the active HE compositions and may open avenues for further research and development of munitions of the future.

1. Introduction

Additive manufacturing (AM) technologies are maturing and allowing effective manufacturing of components, including those of energetic material devices. Conversely, technology advances in AM may also enable more sophisticated fabrication of improvised explosive devices that are hard to detect. Stakeholders within the defence research and development sector need to be aware of this potential threat and strive to develop counter solutions. AM is a broad-spectrum term that includes several technologies that can create 3D objects by adding material layer-by-layer. The benefits of the AM of materials include rapid prototyping, control over the material composition, and cost-effective manufacture of short product runs. The AM processing of energetic materials allows structuring of the material at the mesoscale, something that is challenging to achieve with conventional methods. The material composition can be controlled, the particles can be manipulated from micro to mesoscale and manufactured for unique structures in theatre [1–3].

The rapid development of the additive manufacture technology also affects the field of explosive materials. It has to be accepted that this technology will in future be available to defence forces and adverse insurgent elements alike. It is therefore imperative that proactive research is executed to gauge the potential application of this technology and processes that can be used for energetic material manufacturing. Understanding these processes will enable further research on the effects of emerging high explosive (HE) compositions and devices to provide protection solutions and counter-measures against such threats. Other advantages of AM of explosive devices include:

- a need for precision placement of materials while minimising wastage,

* Corresponding author.
E-mail addresses: jibazetu@gmail.com, Zetu.Jiba@rheinmetall-denelmunition.com (Z. Jiba).
Peer review under responsibility of China Ordnance Society

https://doi.org/10.1016/j.dt.2019.05.013

- unique structures for warheads which are not obtainable by traditional ways,
- control of composition as gradients can produce unique explosive effects,
- improved insensitivity,
- reduced time between design and manufacturing,
- cost-saving and material control, and
- improved logistics as the application facilitates the military to manufacture munitions even in the theatre of operations [3–10].

Currently, the traditional manufacturing methods for explosive devices are limited to production via cast-cure, melt-cast, and pressed powder. High explosives, such as RDX-based composite materials are currently limited to production via the pressed powder method or castable mixtures which require further processing for unusual shapes and which introduce sensitivity and safety issues in the manufacturing process. Furthermore, the processes are difficult and costly to update large-scale preparation plants [1]. PBXs have been commonly used in both military and industry because of their improved safety, enhanced mechanical properties and reduced vulnerability during storage and transportation. The pressed powder processes include explosive powder materials, wax or polymer binder and solvent producing polymer/plastic bonded explosives (PBXs), whereby the energetic particles are first coated with a binder [11–18].

The ability of AM methods such as fused deposition has been demonstrated on pyrotechnics and propellants [19–21]. Components compatible with high explosives have been manufactured through AM methods in the combat theatre as containers for holding the explosive charges [4]. Researchers have attempted the 3D printing process on TNT, a high explosive material, but difficulties in controlling its behaviour and safety issues that arise during and after the process remain a concern [5,9,10]. As such, 3D printing studies of a mock TNT material was executed to control and tailor internal structures for a new explosive form. Gash [5] studied and developed the methodology to produce plastic-bonded high active explosive components for a direct ink-write AM process. The product consisted of 94% (by weight) crystalline explosive agglomerate bonded together with a thermoplastic polymer. There is, however, an increasing need to improve the manufacturing method for high explosives (HEs) to achieve unique shapes that can be produced for different unique detonation and explosion effects. This is the area in which selective laser sintering (SLS), an upcoming AM method envisaged to be for manufacturing energetic material devices, can be of assistance.

Selective laser sintering (SLS) is an additive manufacturing (AM) technology that uses a laser to sinter powdered plastic material into a solid structure based on a 3D model. An infrared laser beam selectively activates target powder particles causing them to partially melt and coalesce with neighbouring particles to form a monolithic layer. However, the particles never reach a fully liquefied state during the sintering process. The adaptation considered presently, is to employ a thermoplastic particle coating with the idea that it will melt and effect the sintering without the HE core melting at all or even be exposed to excessive heat [7,8]. This technique is being considered because it prints very accurate and precise parts compared to other processes, no support structures are required due to the powder bed supporting the part, no post curing is required, and the laser has a fast scanning speed which can be adjusted and reduces printing time, paramount pre-processing to ensure safety during the manufacturing process, prior to sintering with the laser beam, the absorbing material (binder particles) are not completely melted but instead the temperature is raised to just above the glass transition temperature or just below the melting temperature where the material becomes soft and rubbery, there is no risk of clogging such as with the nozzles included in other processes, and larger parts can be printed due to the larger build envelope [4–8].

The ultimate goal is to 3D manufacture intricate explosive components using an RDX-based formulation using SLS technique. A major challenge is the integration of non-castable high explosives such as RDX with the SLS environment. Activation of the RDX during the process must be avoided for both safety and technical reasons. This means that formulation exercise is necessary in order to make high explosives compatible with SLS. For example, individually coating particles decreases RDX sensitivity [22]. Therefore, the idea was to coat the RDX particles with another material, a binder or other suitable explosive, with a much lower melting point than RDX. Desired were composite particles formed by micro-encapsulating individual RDX particles with the binder material [23]. If these can be obtained as near spherical particles, the SLS sintering will rely on the melting of the coating material to effect sintering and coalescence of neighbouring particles into a dense monolithic solid film layer. It must be noted that both porosity and the presence of large amounts of inert materials are undesirable. Their presence will reduce both the energy output and the detonation velocity of the explosive. Therefore, dense prints are the desirable output. For safety and practical reasons, this project used inert simulants to mimic the explosive materials of interest [22–26]. For this initial stage, the primary purpose was to find a functional process that can be used to prepare mock RDX composites additively using the SLS technique.

Because spherical Particles that are 20 μm and larger are preferably deposited in the dry deposition as they tend to flow better [27] and have low internal friction [19,28]. The critical constraints for this work were coating effectiveness, generating spherical particle morphologies, controlling particles size in the micron size range (>20 μm) and binding performance under SLS conditions. The RDX simulant and coating processes investigated are similar to those reported in the literature [12,13,29–32]. The selection of the RDX inert simulant was primarily constrained by the solubility in the solvents used and thermal attributes compared to RDX, with quasi-comparable physical properties. A binder, with a low melting point but fast solidification properties and with a very high IR absorbance at the peak of the laser wavelength band, in contrast to the RDX simulant, was used [33,34]. The proposed formulation method developed, may in future enable safe additive preparation of non-cast HE compositions, and it furthers the research and development of novel munitions.

2. Experimental

2.1. Materials

Poly-ε-caprolactone (PCL) and 3,4,5-trimethoxybenzaldehyde (utilised as TNT simulant) with melting points of 60 °C and 73 °C–82 °C, respectively, were explored as potential coating materials and binders. PCL is a biodegradable polymer used in pharmaceutical research (for particle encapsulation) for improved stability and shelf-life, solubility enhancement and controlled sensitivity. It has been used as an energetic polymer in pyrotechnic compositions. The 3,4,5-trimethoxybenzaldehyde obtained as a light yellow flake and it mimics TNT physical and chemical attributes (except for energetics). The molecular weight is 196.6 g/mol; the density is 1.40 g/cm^3; the melting is virtually the same (84 °C) as that for TNT and decomposition temperature is 337 °C. The binders were obtained from Sigma Aldrich and used as received.

The selection of the RDX simulant was informed by the extent to which they mimicked RDX with respect to its actual thermal and

physical properties, including solubility in organic solvents but highly sparing solubility in water. Potassium bitartrate, purchased from Sigma, was chosen as RDX simulant. It has a melting and decomposition point of 230 °C, the molecular weight is 188.18 g/mol and it has a density of 1.05–1.95 g/cm^3, and it had the required solubility profile. Polyvinyl alcohol (PVA) was used as a stabiliser for the emulsification the formulations. The grade used had a molecular weight of 22000 g/mol and the degree of hydrolysis was 86–88%. Reagent grade dichloromethane (DCM), acetone, cyclohexanone and chloroform were also purchased from Sigma. All chemicals were used without further purification.

2.2. Methodology

The potassium bitartrate particles (RDX simulant) were reduced via a ball milling process and sieved to obtain fine particles with the desired particle size. Desired were near-spherical particles before coating. It was a requirement for the coating methods employed to achieve 1) microspheres larger than 20 μm but still in the micron range, and 2) a free-flowing and non-agglomerated powder for simple deposition and packing during the sintering process [28]. The influence of these constraints (spherical particles, particles size and coating efficiency) were investigated on the SLS process by evaluating their effect on fusion and packing of the coated particles. The powder characteristics affect the sinterability, and also the pore size, surface area, and surface roughness of the final product. The particle size affects the design parameters of both the printing process and the final part. The particle shape and size distribution affect the most important powder properties, i.e. the propensity to flow and deposit. Spherical particles larger than 20 μm are preferred for this application because the corresponding powders have a low internal friction and tend to flow well [29]. As it has been reported, the particle size in the range of 20–100 μm is preferred for the SLS of polymer based particles [35–37]. However, this study is explored the concept beyond 100 μm but still in the micron range. The literature also reports that a way to create a denser sintered layer is to create a more dense bed prior to the sinter [38–40]. This means mixing different sizes or grades of particles and the particle sizes should be designed and mixed in proportion to better fill space in your sinter bed to maintain a heterogeneous packing state well and reduce voids. Research has shown that packing the coarser grains with smaller particles not only yields higher density powders but also decreases balling defects in the finished printed product [38]. The coated particles were sieved through different meshes (50 μm, 80 μm, and 200 μm) and separated in terms of the particles size before SLS. The particles in the range 50–200 μm were the most dominant ones, and hence were sintered with results shown in Fig. 8(c). Two sets of sintered powders were 50–200 μm and the 50–500 μm which also resulted in voids and is not presented for this paper.

2.3. Coating formulations

Inert mock RDX composite particles were obtained via emulsion-based processes as shown on the flow diagram in Fig. 1. The formulations evaluated consisted of potassium bitartrate as the RDX simulant (90 wt% and 60 wt%). The poly-ε-caprolactone was used as a polymeric binder (10 wt%) and 3,4,5-trimethoxybenzaldehyde was used as TNT simulant as an alternative second binder (40 wt%). The objective was to investigate and evaluate these processes for their ability to yield the required spherical micro-particles in the desired size range at high coating efficiencies. Parameters such as the nature of the organic solvent, temperature, pressure, stirring intensity and evaporation method were varied to find suitable conditions for the required end product.

A literature procedure [28,29] was employed to effect the microencapsulation of the RDX simulant with PCL. The suspension system procedure is shown schematically in Fig. 1(a). A 100 mg PCL was dissolved in 20 ml DCM, forming a polymer solution. The RDX simulant powder (900 mg) was dispersed into the PCL solution with stirring maintained at 100–200 rpm. This suspension was stirred into a medium made up of 2 mL of the 1 wt% PVA (used as an emulsifying agent) and 20 ml deionised water. The PVA was utilised to prevented agglomeration of the droplets in the suspension. The resultant suspension was held at 40 °C and stirred continuously for 6 h. During this time the organic solvent was evaporated and the droplets solidified. The resulting microspheres were recovered from the mixture by decanting and dried in an oven at 40 °C for about 24 h.

On the other hand, the microencapsulation of the RDX simulant with the TNT simulant was conducted via a single emulsion process, as shown in Fig. 1(b). The TNT simulant was melted by heating to 90 °C. Then the RDX simulant particles were dispersed into the melt by homogenising at 800 rpm for 2 min. The emulsification was achieved using IKAT25 Ultra-Turrax homogeniser. Next 40 mL deionised water was added while maintaining the temperature at around 90 °C at a reduced stirring speed of ca. 200 rpm for 10 min using a magnetic stirrer. The temperature was then reduced to 23 °C with stirring for 30 min to obtain droplet microspheres suspended in cooled water. The microspheres were dried in the oven at 50 °C for about 8 h to remove residual water.

2.4. Characterisation

The particle size and morphology were investigated by imaging on a Zeiss Crossbeam 540 FEG Scanning Electron Microscope (SEM) operated between 1 kV and 3 kV. Attenuated total Reflection-Fourier transform infrared spectroscopy (ATR-FTIR) spectra were recorded on an in-house PerkinElmer Spectrum 100 Series instrument. The recording was done at 32 scans over the wavenumber range 500–4000 cm^{-1}. High-resolution confocal Raman imaging was carried out using a WITec alpha 300 RAS + confocal Raman microscope and a 532 nm excitation laser at low power of 1 mW. The surface image scans were acquired using a 50 × /0.75 Zeiss objective which gives a diffraction limited lateral resolution of 433 nm, and the scans were acquired over 40 × 40 μm^2 area with 150 points per line and 150 lines per image using an integration time of 1 s. Differential scanning calorimeter (DSC) runs were conducted on a TA Q100 instrument under a nitrogen atmosphere. The temperature was scanned from −80 °C to 100 °C at a ramp rate of 10 °C/min. This was done to determine the thermal attributes of the coatings present on the samples, i.e. the melting point, enthalpy change and crystallinity on the coated samples. Laser sinterability was explored with a Synrad CO_2 Infrared (IR) laser (model D48-2-28w). The laser wavelength was 10.6 μm, the spot size was 2 mm, and the laser power was varied from 0.5 to 3 W.

3. Results and discussion

Fig. 2 shows the uncoated simulant used in the formulations with a narrow particle size distribution and with a reasonable Malvern particle sphericity after sieving. The order of sphericity (roundness) of the sieved uncoated particles is demonstrated in Fig. 2(b). The analysis was conducted using a Malvern particles morphology. The closer to the order of 1 the particle gets, the closer it is to a spherical shape. Fig. 3(a) shows SEM micrographs of PCL coated particles, obtained with the suspension method. The coated particle size ranged from 50 μm to 500 μm, i.e. it was comparable in size to RDX production grade (A) as a fine crystalline material as

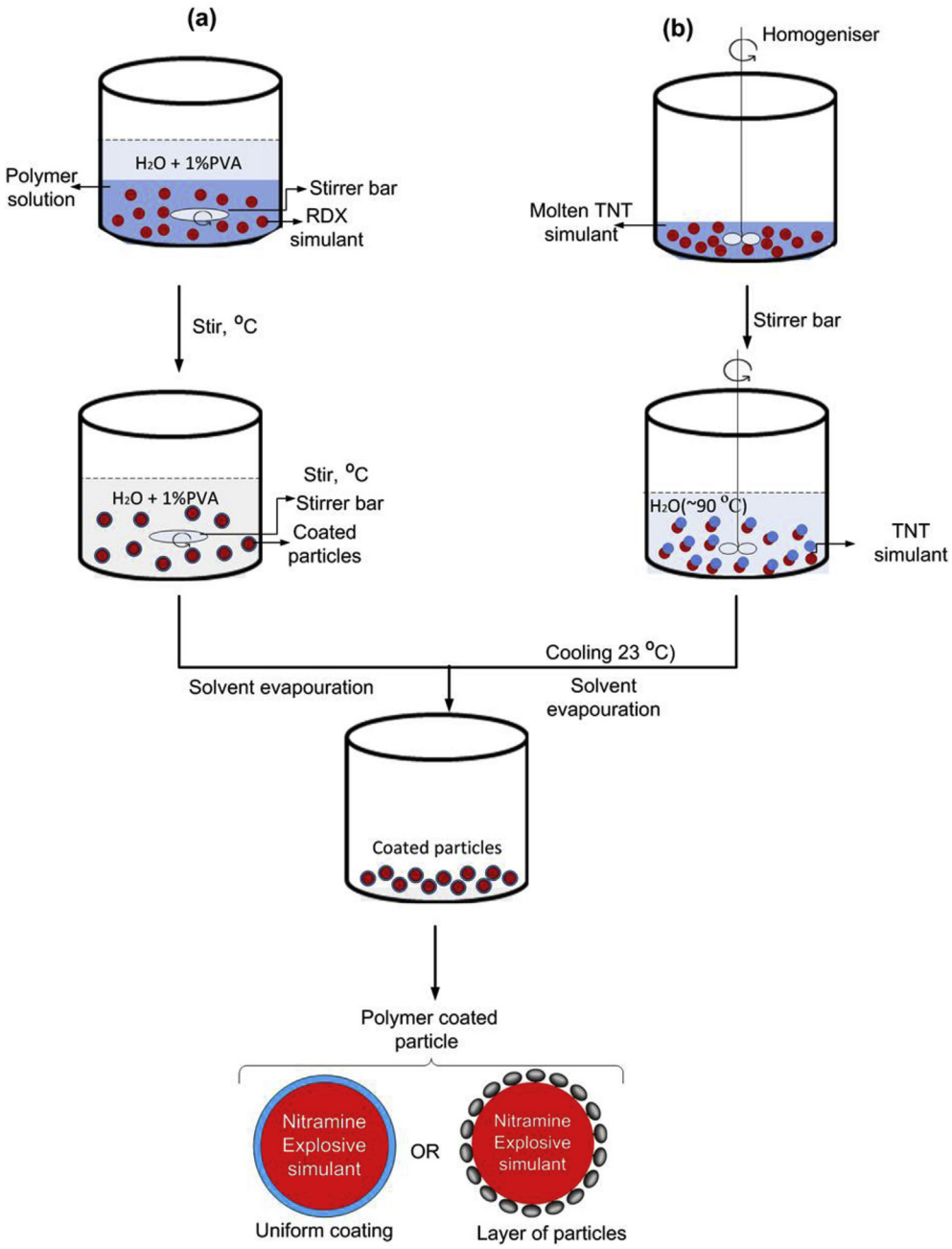

Fig. 1. Schematic of the emulsion-based microencapsulation procedures used for the preparation of mock RDX/TNT microspheres: Potassium bitartrate as RDX simulant with (a) 10 wt% poly (ε-caprolactone) as binder, and (b) 40 wt% 3,4,5-trimethoxybenzaldehyde as TNT simulant.

reported in the literature [33,34]. To determine the coating thickness, the coated particles were imbedded by Resin on a substrate. An Ultra-microtome cutting method was used to section the coated particles in half. The micrographs of cross-sectioned particles are shown in Fig. 3(b) with coating thickness around 7 mm. Fig. 4(b) shows a micrograph of the cross-section of the PCL coated particle, showing details of the core material and the coating forming the outer shell.

Fig. 4 shows the TNT simulant coating on the RDX simulant particles. Because the interest lies in the particle shape, size and coating, the images are shown at different magnifications for clarity. The particle size ranged from 100 μm to 700 μm. The particles featured a near-spherical morphology with a rough but uniform surface. It can be observed that the microgranule consists of a cluster of smaller particles. Such structural configuration is evidence that the granules formulated possess compact smaller particles with fairly low porosity. This a potential good application for firepower, as it is reported that individually coated particles decrease sensitivity and smaller explosive particles organised into clusters that maintain the same structure drastically increase weapon safety and performance [17,22]. Additionally, larger particles (formed of smaller particles) are easier to spread during SLS and thus potential advantage of increased sinterability and aid in the production of more homogeneous parts [41,42]. Fig. 4 (a and b) shows close-up detail of the surface. Fig. 4 (c and d) show the confocal Raman intensity mapping acquired from the surface and

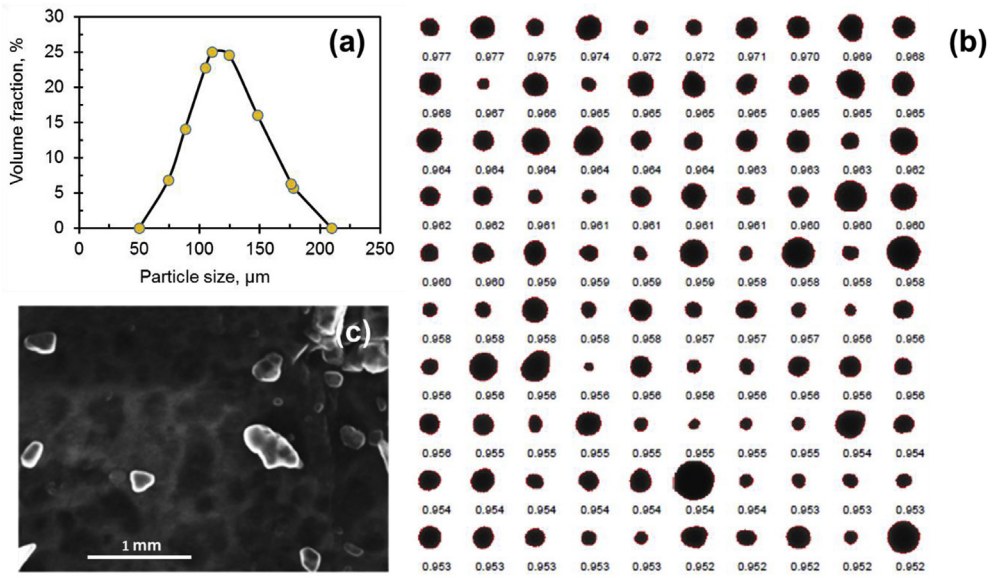

Fig. 2. Uncoated RDX simulant (Potassium bitartrate): (a) Particle size distribution, (b) Malvern particle morphology in order of sphericity after sieving process, and (c) SEM image showing the particle morphology before processing.

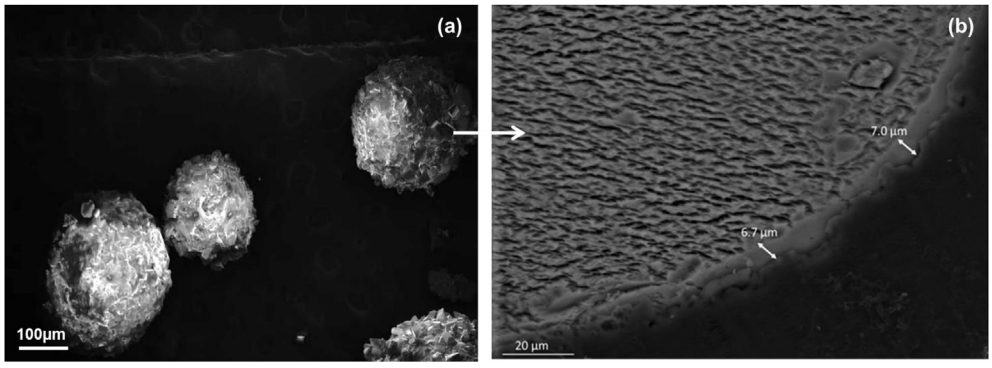

Fig. 3. Mock RDX/PCL at magnification (a) and (b) Photomicrograph of coated particle cross-section of the mock showing the coating thickness.

core of the RDX/TNT mock, respectively.

The mapping was carried out over a large area of $40 \times 40\ \mu m^2$ and 150×150 Raman spectra were acquired over a shift of $0–3800\ cm^{-1}$ (see the average Raman spectra in Fig. 6(a)). From the average Raman spectrum of the surface and core of the RDX/TNT mock, it can be seen that most peaks overlap. However, the peak at $883\ cm^{-1}$ from the core spectrum does not overlap with those from the surface spectrum of the mock. Similarly, the peak at $1585\ cm^{-1}$ from the surface spectrum does not overlap with those from the core spectrum of the mock. As a result, these peaks were used to distinguish the surface and the core of the RDX/TNT mock and to evaluate the uniformity of the chemical composition of the microspheres, as shown in Fig. 4 (c and d).

A nearly uniform intensity of the mapping suggests a uniform chemical composition (phase) of TNT coating on RDX core across the analysed areas of the surface and core of the mock. An observed slight variation in the confocal Raman intensity of the mapping is due to the irregular surfaces of the analysed areas which cause variation in the microscope focal plane during analysis. It was deducted that the formation of these microspheres depends on the slow rate of stirring (around 200 rpm) and evapouration method. Drying or evaporation temperatures around 40 °C–50 °C and ambient pressure were the key. The literature [30,31,43] also reports that the stirring speed between 100 and 250 rpm at evapouration temperatures 40 °C–60 °C affects particle size diameter ranging from 20 to 200 μm for coated microspheres. However, it was noted during the experiment that the slow stirring (100–250 rpm) at temperatures between 40 °C and 60 °C influences microspheres in the region of 50–700 μm, made of a particle cluster.

FTIR was used primarily to assess and confirm the presence of the binder and to confirm the strong absorbance of the molecules in the coating material at the laser wavelength [44]. It was, therefore, paramount to show the presence of the binder as a coating material in these inert mock composites. Fig. 5(a) and Fig. 5(b) shows the FTIR spectra for the RDX simulant and the coating materials (binders) as references together with the coated samples (inert mock composites). There are some clear observations that can be made, the peak intensities of the binders' stretching frequencies are comparable with the coated samples.

The peak around $3340\ cm^{-1}$ due to the RDX inert simulant molecule (O–H) is observed on all coated samples and correlates with the mid-IR laser wavelength (2.9 μm). The unique double peak around $2900\ cm^{-1}$ (corresponding to 3.5 μm mid-IR wavelength) due to CH_2 (single peak due to C–H) stretch on both the PCL and 3,4,5-methoxybenzaldehyde spectrum is observed on the coated

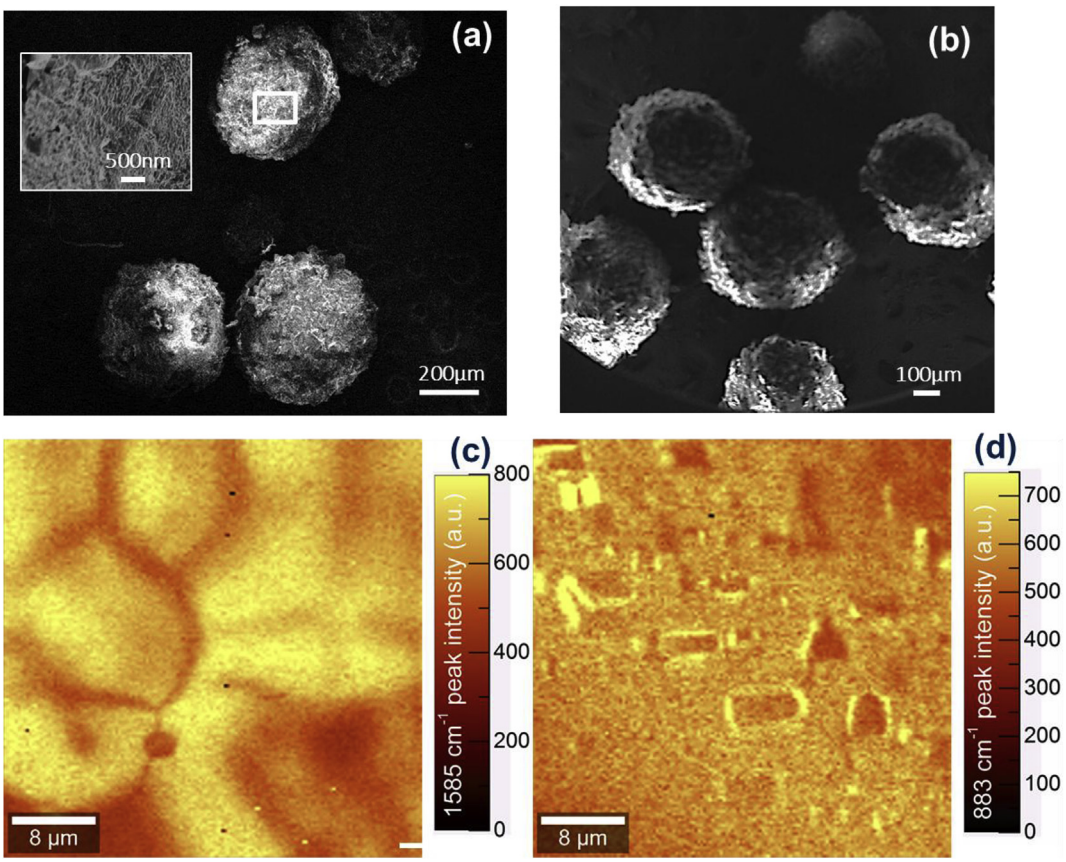

Fig. 4. SEM images at low magnification (a) 200 µm, (b) 100 µm, (c) Surface microstructure of the mock RDX/TNT granule, confocal Raman intensity mapping of the 883 and 1585 cm^{-1} peaks of the microsphere (c) core and (d) surface.

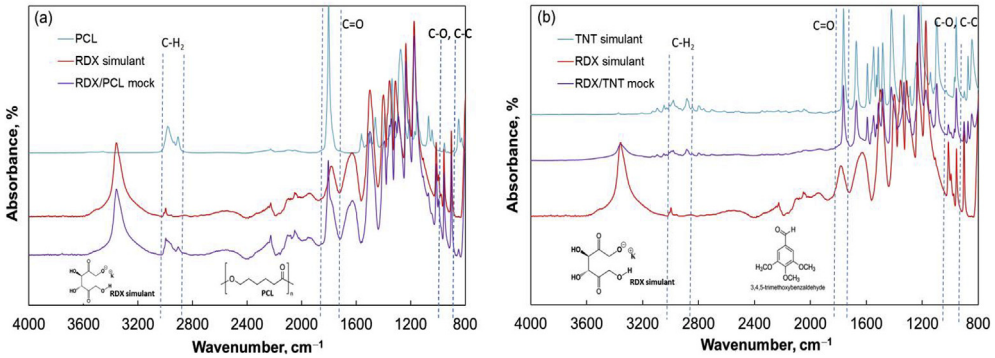

Fig. 5. FTIR characterisation of mock explosive formulations.

samples. The simulant also indicates a weak stretching frequency of C–H. The region around 1800 cm^{-1} absorbing area on the coated samples is also observed due to RDX simulant acidic C=O- stretch and a strongly absorbing PCL (ester C=O- stretch). Another strong stretching frequency peaking around 1700 cm^{-1} is due to the TNT inert simulant used as a binder. This is also close to the carbonyl stretching frequency of the RDX simulant. These frequencies correlate to a far-IR laser wavelength (from 5.5 µm) and may not be suitable if the only intention is to activate the binder. Therefore, the best laser wavelength to possibly only activate the binder materials would be around 3.5 µm (due to the CH_2 stretch), the mid-IR laser wavelength.

However, the RDX is reported to be less active and its molecules (such as NO_2, C–H) do not absorb energy in the IR wavelength region. Hence the IR cannot break the chemical bonds of the active molecules to induce the exothermic reaction [45]. From the safety standpoint, this is a good attribute on RDX for the SLS process. Additionally, the RDX does not form a plasma (which may influence ignition of the material) when exposed to energy from the IR wavelengths [44–47]. Therefore, the sintering and fabrication process of active RDX composites may be possible with the whole IR wavelength regime (up to 10.6 µm) as the source of energy.

The chemical vibrational modes were confirmed by the Raman chemical shift analysis, that suggest the similarities of the chemical phases possessed by the coated samples compared to the starting materials. Fig. 6 shows the Raman spectra of the starting materials

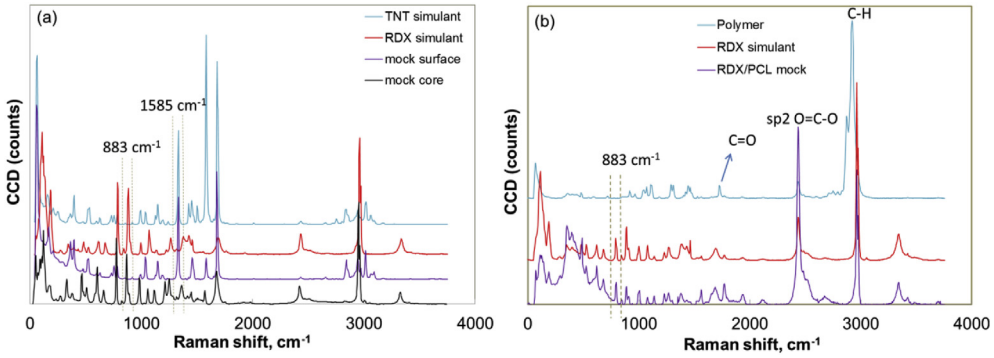

Fig. 6. Raman characterisation mock explosive formulations.

and the mixture (both the mock particle surface and the core presented). The Raman shifts are in agreement with the chemical shifts observed in FTIR spectra. The shifts of the core for the granules seem to be correlating with those of the RDX simulant as highlighted on Fig. 6(a) around 250 cm^{-1}, 900 cm^{-1} and 3000 cm^{-1}. The shifts measured on the coated particle surface compare more with the TNT inert simulant. Fig. 6(b) confirms the uniqueness of the CH_2 shift (2900 cm^{-1}) influenced by the PCL binder observed on all coated samples. There seem to be other common effects around 400-500 cm^{-1} and 2400 cm^{-1} (influenced by O–C=O group) indicating that the coated samples do comprise both starting materials.

It is further observed on the DSC heat curves in Fig. 7(a) that all the coated samples possess an endothermic peak around 60 °C (absent in the simulant spectrum) due to the melting point of PCL. While Fig. 7(b) shows the thermal attributes on the coated RDX inert simulant particles comparable with 3,4,5-trimethoxybenzaldehyde (TNT simulant). These thermal attributes (endotherm and exotherm) are absent for the neat inert simulant. This confirms the presence of binder materials in the coated samples and that it is possible to activate or soften the binders around their melting points and crystallise at cooling without affecting the simulant. Assuming that the crystallinity of the binder in the coated samples is still the same as before formulation; the binder content is about 9.2% in the sample for PCL -coated particles and about 32% in the simulant TNT-coated particles.

3.1. Selective laser sintering tests on coated mock formulations

The formulated mocks were sintered to assess the viability of the inert RDX simulant particles being fused and bonded by a polymeric binder and TNT simulant via the SLS method. This was conducted on a pre-placed direct laser sintering process. The aim was for the binder to only absorb the laser energy and get activated to allow coalescence and sintering at cooling.

Initial studies were performed on the binder particles to show that they can indeed absorb the IR wavelength and that it is actually possible to perform SLS. The optical micrographs of the sintered layers are shown in Fig. 8(a) and Fig. 8(b). Fig. 8(c) shows the sintered area, giving details to the contact between bonded particles, voids and the thin coating. It can be observed that the bonding between the PCL-coated particles was well facilitated. It was anticipated that the formulation methods may either produce a uniform coating or a layer of particles. It was then observed that the coating on the surface is uniform and not in a form of “layer of particles”. Hence the effect of the latter was not determined. Moreover, the uniform coating does influence a good sintering mechanism. The interior void spaces are confirmed on the sintered mock. These voids may affect the explosive performance (density) of the real active end product depending on the particle size relative to the void size. Smaller voids relative to the solids should not be a critical factor in explosives. However, since it is reported that large structures of RDX without voids do not allow sufficient hot spots for a shock stimulus to generate the conditions needed to start and sustain a chemical reaction [27]; hence the voids can be allowed on condition that they are smaller relative to the EM particles. Additionally, during SLS printing, there must be enough binder to fill the open spaces between closed packed core particles. Otherwise, the overall component will not be void free. Hence the presence of voids is inevitable with a small binder ratio in the formulation. Increasing the inert binder (polymer) may, however, decrease the performance of the active core. For the PCL coated particles, the sintering was achieved from minimum 0.5 W IR laser power with a focused beam of about 1.8 mm spot size at minimum exposure time of 15 s. This exposure time was validated sufficient to facilitate the bonding between the coated particles without decomposing the polymer. The testing of sufficient power was

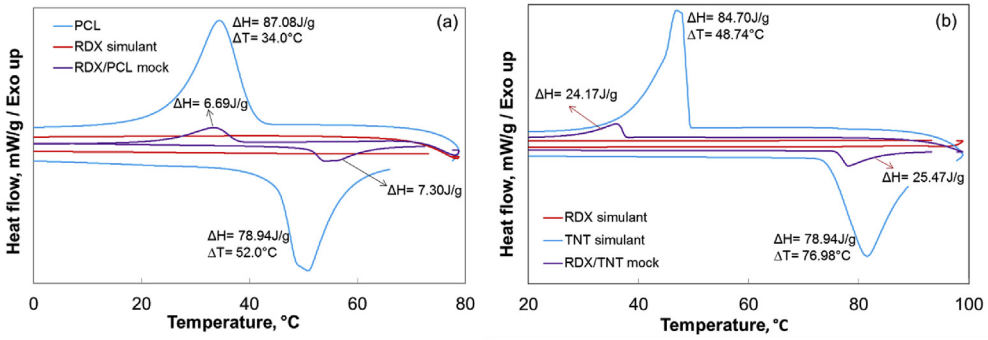

Fig. 7. DSC analysis of the HE inert mock composites, (a) PCL coated particles and (b) TNT inert simulant coated particles.

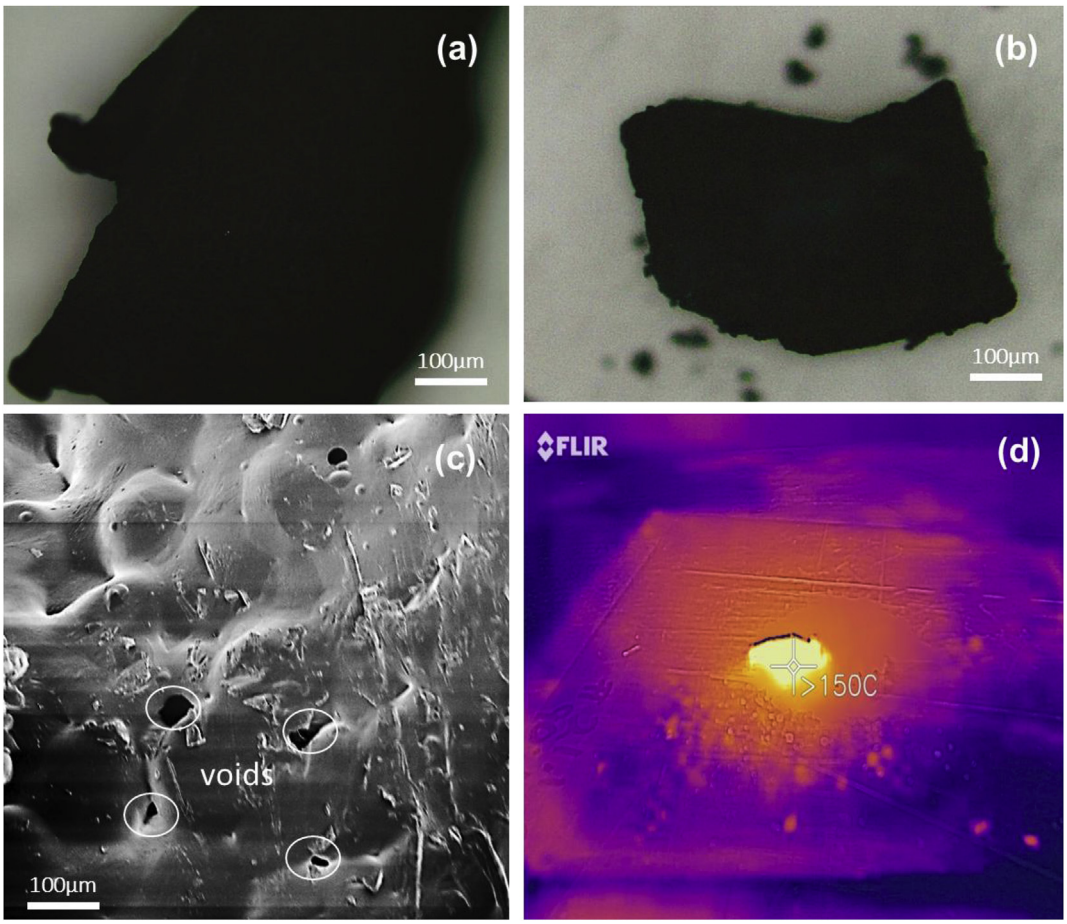

Fig. 8. (a) and (b) Optical micrograph of a sintered PCL and TNT simulant, (c) SEM images of sintered mock (layer) from PCL coated RDX simulant particles, (d) High speed image of RDX/TNT mock showing the decomposed TNT simulant area after exposure to solar energy SLS.

functional from minimum laser power 0.5 W–3 W and 15 s exposure time. The polymer was only observed to decompose at higher laser power above 3 W for longer exposure times. However it is understood that the laser power does fluctuates at lower powers around 0.5 W. Hence the power should be above 0.5 W. The sintered layer appears to possess a homogeneous smoother surface compared to prior sintering.

However, the mock RDX/TNT did not sinter using the IR wavelength. This is possibly due to the TNT simulant absorbing energy insufficiently around the wavelength used. Moreover, when exposed to the solar energy SLS, it still did not sinter but the coated particles decomposed around 150 °C, as can be observed in Fig. 8(d). In solar energy SLS, The SLS system used the energy harnessed form the solar radiation as the source of energy to sinter the material. The sun rays were concentrated and focused with a Fresnel lens. It was then concluded that the TNT simulant is not suitable for SLS as the AM technique, and hence the real TNT may not be conducive for this technique environment. Therefore, another AM technique should be considered for this formulation.

The packing density of both mock composites was calculated using the rule of mixtures and it is estimated to be 1.20 g/cm^3 [24]. The density of PCL-bonded real active RDX was estimated from the theory of random packing of spheres [48], to be around 1.57 g/cm^3, comparable to that of C4 and PE4 as a PBX produced from a traditional press powder method. The density of TNT-coated RDX was also estimated around 1.64 g/cm^3 which also comparable to that of composition B explosive mixture. For this proof of concept, only one sintered layer was formed as a pre-placed sintering method (manual) was used. Determination of the packing density, experimentally, shall be conducted in the follow-up study on optimization of these methods on active materials.

4. Conclusion

The purpose of this project was to investigate and evaluate coating processes to enable SLS of polymer-bonded explosives and high explosive (HE) composites. This was primarily conducted through a demonstration of the concept by use of inert simulants and thus mocks for safety and practicality reasons. Suspension systems and single emulsion were investigated (varying the input parameters) for required coated microspheres, uniform coating effectiveness and bonding or sintering performance under a selective laser sintering method. The resultant PCL coated microspheres possessed a uniform coating. The microspheres coated with inert simulant TNT comprised compact particles and uniform coating with fairly rough surface. The suspension and single emulsion processes were found to produce mock powder particles with required constraints such as spherical morphology, required size range (>20 µm) with uniform but rough coating surface. The SLS concept was demonstrated successfully for the PCL coated mock. Preliminary binding experiments indicate that laser sintering with IR wavelength for PCL coated RDX simulant particles from the suspension process is plausible according to the bonding mechanism of the coated particles regardless of the voids formed. On the other hand, the TNT inert simulant coated RDX simulant (RDX/TNT mock) is found to be incompatible and unsuitable with

the SLS technique.

It is therefore recommended that non-laser energy based additive manufacturing techniques such as binder jetting be tried for this formulation. Further research within this project aims to investigate the suspension and single emulsion processes as coating formulations with already determined parameters using the actual active RDX and further characterise the composites for performance and safety for the SLS. The results from this approach will be used to compare with the PBXs from the traditional methods.

Acknowledgements

This is the research initial study funded by the Council for Scientific and Industrial Research (CSIR), no grant number. The authors would like to thank the University of Pretoria Microscopy Laboratory, the CSIR Polymer and Composite Unit, and the CSIR NLC for the help received in the Laboratories. We would also like to extend our gratitude to Paul Sonnendecker in Chemical Engineering, University of Pretoria, for assisting with the solar system SLS test.

References

[1] Emery S. REVIEW : traditional manufacturing of explosives. Distributi; 2015. doi:IHEODTD 16-061.
[2] Matt Thomas. The magic of rapid prototyping for user research: much more than smoke and mirrors. January 30 2014.
[3] Murray AK, Isik T, Ortalan V, Gunduz IE, Son SF, Chiu GTC, et al. Two-component additive manufacturing of nanothermite structures via reactive inkjet printing. J Appl Phys 2017;122:1–6. https://doi.org/10.1063/1.4999800.
[4] Lawrence Livermore National Laboratory. 3D printing of energetic materials and components for optimized or enabling technologies. n.d. https://ipo.llnl.gov/technologies/energy_materials.
[5] Gash A. High-explosive components using advanced manufacturing methods. Lawrence Livemore Natl Lab; 2015.
[6] Hutterer E. Explosives 3D printing 2016:2–5. https://www.lanl.gov/discover/publications/1663/2016-march/_assets/docs/1663_26_explosive-3d-design.pdf. [Accessed 27 June 2018].
[7] Saffarzadeh M, James Gillispie G, Brown P. Selective laser sintering (sls) rapid protytping technology: a review of medical applications 2016.
[8] Bakshi KR, Mulay AV. A review on selective laser sintering: a rapid prototyping technology. In: IOSR J Mech Civ Eng 53 Page MES Coll Eng; 2016. https://doi.org/10.9790/1684-15008040453-57 LK -. 2278–1684, https://aus.on.worldcat.org/oclc/6682027765.
[9] Kerns Jeff. A look inside the “explosive” 3D-printing industry n.d. 2018. http://www.machinedesign.com/3d-printing/look-inside-explosive-3d-printing-industry.
[10] Los Alamos Science and Technology Magazine. 3D-printed explosives Fine-tuning microbial metabolism New tamper-evident seals tell all Breaking bacterial defenses. Los Alamos Natl Lab 2016;2–29.
[11] Yang Z, Ding L, Wu P, Liu Y, Nie F, Huang F. Fabrication of RDX , HMX and CL-20 based microcapsules via in situ polymerization of melamine – formaldehyde resins with reduced sensitivity, vol. 268; 2015. p. 60–6.
[12] Hunt EM, Jackson M. Coating and characterization of mock and explosive materials. Adv Mater Sci Eng 2012;2012:5. https://doi.org/10.1155/2012/468032.
[13] Elizabeth DCM, Moreira ED, Diniz MF, Dutra RCL, Da Silva G, Iha K, et al. Characterization of polymer-coated RDX and HMX particles. Propellants, Explos Pyrotech 2008;33:44–50. https://doi.org/10.1002/prep.200800207.
[14] An CW, Li FS, Song XL, Wang Y, Guo X De. Surface coating of RDX with a composite of TNT and an energetic-polymer and its safety investigation. Propellants, Explos Pyrotech 2009;34:400–5. https://doi.org/10.1002/prep.200700286.
[15] An CW, Guo XD, Song XL, Wang Y, Li FS. Preparation and safety of well-dispersed RDX particles coated with cured HTPB. J Energetic Mater 2009;27:118–32. https://doi.org/10.1080/07370650802405265.
[16] Siviour CR, Gifford MJ, Walley SM, Proud WG, Field JE. Particle size effects on the mechanical properties of a polymer bonded explosive. J Mater Sci 2004;39:1255–8. https://doi.org/10.1023/B:JMSC.0000013883.45092.45.
[17] Thelma G.Manning and Bernard Strauss. Reduction of energetic filler sensitivity in propellants through coating. US 6,524,706 B1, 2003.
[18] Stepanov V, Anglade V, Balas Hummers WA, Bezmelnitsyn AV, Krasnoperov LN. Production and sensitivity evaluation of nanocrystalline RDX-based explosive compositions. Propellants, Explos Pyrotech 2011;36:240–6. https://doi.org/10.1002/prep.201000114.
[19] Bouffard J, Bertrand F, Chaouki J, Giasson S. Control of particle cohesion with a polymer coating and temperature adjustment. AIChE J 2012;58:3685–96. https://doi.org/10.1002/aic.13765.
[20] Scheck Caroline E, Wolk Jennifer N, Frazier William E, Mahoney Brian T, Morris Kyle, Kestler Robert, Bagchi A. Naval additive manufacturing: improving rapid response to the warfighter. Nav Eng J 2016;128:5.
[21] Tappan AS, Ball JP, Colovos JW. Inkjet printing of energetic materials: Al/MoO3 and Al/Bi2O3 thermite. Proc Int Pyrotech Semin 2012;38th:605–13.
[22] Wejsa J. ARDEC energetics. In: ARDEC Energ. Jt. Armaments Conf.; 2010. p. 1–16.
[23] Konek C. Terahertz spectroscopy of explosives and simulants: RDX, PETN, sugar, and L-tartaric acid. SPIE Defense 2009;7311. https://doi.org/10.1117/12.817913. 73110K–73110K–7.
[24] Yeager JD, Higginbotham Duque AL, Shorty M, Bowden PR, Stull JA. Development of inert density mock materials for HMX. J Energetic Mater 2018;36:253–65. https://doi.org/10.1080/07370652.2017.1375049.
[25] Bardenhagen SG, Luo H, Armstrong RW, Lu H. Detailed characterization of PBX morphology for mesoscale simulations. AIP Conf Proc 2012;1426:637–40. https://doi.org/10.1063/1.3686359.
[26] Hoffman DM, Cunningham BJ, Tran TD. Mechanical mocks for insensitive high explosives. J Energetic Mater 2003;21:201–22. https://doi.org/10.1080/713770433.
[27] Marraud C (Chevanceaux), FR) SM (Le H, (Pessac FC, (Begles) CA. Desensitization by coating crystals of explosive energy substances, coated crystals of such substances, and energy materials. US 20100307648A1, 2010.
[28] Lee B, Jeong J, Lee Y, Lee B, Kim H, Kim H, et al. Supercritical antisolvent micronization of Cyclotrimethylenetrinitramin : influence of the organic solvent. 2009. 11162–7.
[29] Staymates M, Fletcher R, Staymates J, Gillen G, Berkland C. Production and characterization of polymer microspheres containing trace explosives using precision particle fabrication technology. J Microencapsul 2010;27:426–35. https://doi.org/10.3109/02652040903367335.
[30] Jain RA. The manufacturing techniques of various drug loaded biodegradable poly (lactide- co -glycolide) (PLGA) devices. Biomaterials 2000;21:2475–90.
[31] Arshady R. Preparation of biodegradable microspheres and microcapsules: 2. Polyacides and related polyesters. J Control Release 1991;17:1–22. doi:ADONIS016836599100038u.
[32] PANT A, Amiya KN. Preparation and characterization of ultrafine RDX. Cent Eur J Energ Mater 2013;6:19–21.
[33] Trzcinski T, Palka N, Szustakowski M. THz spectroscopy of explosive-related simulants and oxidizers. Bull Pol Acad Sci Tech Sci 2012;59:445–7. https://doi.org/10.2478/v10175-011-0056-4.
[34] Ahmad RS, Cartwright M. Laser ignition of energetic materials. WILEY; 2014. p. 256–8.
[35] Zhu W, Yan C, Shi Y, Wen S, Liu J, Shi Y. Investigation into mechanical and microstructural properties of polypropylene manufactured by selective laser sintering in comparison with injection molding counterparts. J Mater 2015. https://doi.org/10.1016/j.matdes.2015.05.043.
[36] Yuan S, Shen F, Bai J, Kai C, Wei J, Zhou K. 3D soft auxetic lattice structures fabricated by selective laser sintering : TPU powder evaluation and process optimization. Mater Des 2017;120:317–27. https://doi.org/10.1016/j.matdes.2017.01.098.
[37] Yuan S, Shen F, Chua CK, Zhou KSC. Prog Polym Sci 2018. https://doi.org/10.1016/j.progpolymsci.2018.11.001.
[38] Abu-lebdeh T, Damptey R, Lamberti V, Hamoush S. Powder packing density and its impact on SLM-based additive manufacturing. Springer International Publishing; 2019. https://doi.org/10.1007/978-3-030-05861-6.
[39] Karapatis NP, Egger G, Gygax P, Glardon R. Optimization of powder layer density in selective laser sintering. 1999. p. 255–64.
[40] Jacob G, Donmez A, Slotwinski J, Moylan S. Measurement of Powder bed density in powder bed fusion additive manufacturing processes, vol. 27; 2016. https://doi.org/10.1088/0957-0233/27/11/115601.
[41] Utela B, Storti D, Anderson R, Ganter M. A review of process development steps for new material systems in three dimensional printing (3DP). J Manuf Process 2008;10:96–104. https://doi.org/10.1016/j.jmapro.2009.03.002.
[42] Mattos EC, Diniz MF, Nakamura NM, Dutra R de CL. Determination of polymer content in energetic materials by FT-IR. J Aerosp Technol Manag 2009;1:167–75. https://doi.org/10.5028/jatm.2009.0102167175.
[43] Yadroitsev I, Bertrand P, Grigoriev S, Antonenkova G, Smurov I. Use of track/layer morphology to develop functional parts by selective laser melting. J Laser Appl 2014;25:052003. https://doi.org/10.2351/1.4811838.
[44] Ngo TD, Kashani A, Imbalzano G, Nguyen KTQ, Hui D. Additive manufacturing (3D printing): a review of materials, methods, applications and challenges. Compos Part B Eng 2018;143:172–96. https://doi.org/10.1016/j.compositesb.2018.02.012.
[45] Chen Ming-Wei, You Sizhu, Suslick Kenneth S, DDD. Hot spot generation in energetic materials created by long-wavelength infrared radiation. Appl Phys Lett 2014;104.
[46] Gottfried JL, Lucia FC De. Ultrafast laser heating of RDX and polyethylene. 2013. p. 1–33.
[47] Aluker ED, Krechetov AG, Mitrofanov AY, Zverev AS, Kuklja MM. Understanding limits of the thermal mechanism of laser initiation of energetic materials. J Phys Chem C 2012;116:24482–6. https://doi.org/10.1021/jp308633y.
[48] Henry Cohn. Sphere packing 2015:14.